The Las Campanas/AAT Rich Cluster Survey

Eileen O'Hely[1], Warrick J. Couch[1], Ian Smail[2], Alastair C. Edge[2]
and Ann Zabludoff[3]

[1]Department of Astrophysics and Optics, School of Physics,
University of New South Wales, NSW 2052, Australia
eoh@edwin.phys.unsw.edu.au, wjc@edwin.phys.unsw.edu.au

[2]Department of Physics, University of Durham, South Rd,
Durham, DH1 3LE, UK
ian.smail@durham.ac.uk, ace@durham.ac.uk

[3]UCO/Lick Observatory and Board of Astronomy and Astrophysics,
University of California at Santa Cruz, Santa Cruz, CA 95064, USA
aiz@ucolick.org

Abstract: Some unsolved cosmological questions remain in relation to the formation of structure in the universe. One way of addressing such questions is to use rich galaxy clusters as tracers of the growth of large-scale structure. To date, studies of rich clusters of galaxies have concentrated on systems generally at either high redshift or in the local universe. The properties of clusters and their constituent galaxies at these extrema are becoming well understood. In particular, it is becoming clear that rich clusters have undergone considerable evolution both dynamically and in their galaxy populations over the last 5–8 Gyr. We are undertaking a detailed study of rich clusters of galaxies in the range $0\cdot05 \lesssim z \lesssim 0\cdot15$. Our results will be directly comparable to those of previous studies both at high and low redshift and, for the first time, provide continuous coverage across this important and unexplored transitory epoch in terms of galaxy evolution and structure growth.

1 Introduction

Rich clusters of galaxies are fundamental cornerstones of the large-scale structure seen throughout the universe. They are massive ($M \simeq 10^{15}\ M_\odot$), dense systems seen on scales of megaparsecs, which appear to be at the intersections of the filaments, chains and sheets that characterise the large-scale structure of galaxies. Therefore they are clearly central to the growth of large-scale structure and thus are ideal laboratories for studying this process. Furthermore, because they contain rich collections of galaxies all at the same distance and within a relatively small region of sky, they provide a very efficient means for studying volume-limited samples of galaxies and investigating the effects that the high-density environment has on galaxy evolution.

Most of our knowledge of clusters has come from intensive studies of those in the local universe, in particular a small number of very well studied examples such as the Coma and Virgo clusters. Much research has been devoted to understanding the distribution and morphologies of galaxies within these clusters and the overall cluster dynamics (for a recent review see Bahcall 1997). Nearby, regular clusters are dominated by elliptical and S0 (early-type) galaxies (cf. 70% late-type galaxies in the field; Bahcall 1997), and their cores are almost completely devoid of star-forming galaxies. These observations shaped the classical view of clusters being relaxed systems whose galaxies have been inactive in star formation for a large fraction of a Hubble time. However, pioneering work by Butcher & Oemler (1978) showed that clusters at redshifts $z \sim 0\cdot4$ had significant numbers of blue galaxies in their cores compared to their present day counterparts. This effect—commonly called the 'Butcher–Oemler' effect—is now known to be a general property of rich, compact clusters at $z \geq 0\cdot2$, with a clear trend for the blue galaxy fraction to increase with redshift (Couch 1981; Butcher & Oemler 1984).

The high resolution capabilities of the Hubble Space Telescope (HST) has enabled detailed morphological studies of cluster galaxies at high redshift. Recent results from Couch et al. (1998) and Dressler et al. (1997) show that the blue population consists primarily of late-type spirals, a number of which are undergoing dynamical interactions and merging. One popular scenario for the origin of this population is dynamical infall, the blue galaxies being

field spirals which, through their encounter with the intracluster medium and strong gravitational field, undergo enhanced star formation before being morphologically transformed into S0s (Abraham et al. 1996; Smail et al. 1997). Evidence has also been found that the end-products of this process may still be seen in the outer regions of nearby clusters, with Caldwell et al. (1993) finding galaxies with the same post-starburst spectral signatures of the distant cluster populations in the outskirts of the Coma cluster.

Such low-redshift studies have also revealed quite clear evidence of clusters having undergone significant dynamical evolution at recent epochs. This has been through the detection of significant substructure in the velocity and mass distributions within clusters, as traced by their galaxies' dynamics (Colless & Dunn 1996), their hot X-ray gas (White et al. 1993) and their gravitational lensing of background sources (Fort & Mellier 1994). A particularly striking example of this was published by Zabludoff & Zaritsky (1995; hereafter ZZ95), who demonstrated the power of combining spectroscopic redshifts with X-ray imaging to study the dynamical state of Abell 754. Their extensive study revealed a bimodal galaxy distribution which was significantly offset from the X-ray emission, consistent with the displacement seen during the collision of two subclusters in hierarchical clustering simulations (Evrard 1990). During such a collision, the models predict that the collisional X-ray gas is stripped from the free-streaming dark matter and galaxies, and remains out of hydrostatic equilibrium with the dark matter potential for $\sim$1–2 Gyr afterwards. Furthermore, the frequency of such subclustering and merging at a particular epoch is sensitive to the mean mass density parameter, Ω_0 (Richstone et al. 1992; Lacey & Cole 1993). A low-Ω_0 universe has an early epoch of rapid cluster formation, with more regular, spherically symmetric systems at recent times (Evrard et al. 1993), while a high-Ω_0 universe has cluster formation (via subcluster merging) occurring just at recent times.

The fact that the epoch of rapid cluster galaxy evolution coincides with one of major cluster dynamical evolution raises the very interesting question: to what extent is the former driven by the latter? To address this question, we are undertaking a major survey of rich clusters in the redshift interval $0 \cdot 05 \lesssim z \lesssim 0 \cdot 15$. The aim is to track cluster galaxy evolution and cluster dynamical evolution in tandem over this important transitionary interval in look-back time, thereby bridging the gap between the distant and present-day cluster studies. In addition, it is an interval where a large, homogeneous and representative sample of clusters can be compiled and studied through X-ray selection. By studying a statistically significant number of clusters, and thus a representative sample of the cluster population, we shall be able to draw robust conclusions on the overall subcluster merging rate within clusters at this late epoch, and thus place useful constraints on Ω_0.

The outline of this paper is as follows. In Section 2 we outline the design of our study, its scientific goals and the selection of our cluster sample. The specific observations being undertaken for this project are described in Section 3. We conclude the paper by presenting some initial results in Section 4.

2 Design and Goals of Study

2.1 Overview

Our primary objective is to determine the evolutionary status of clusters—both in the dynamic and galaxy population sense—within the range $0 \cdot 05 \lesssim z \lesssim 0 \cdot 15$. The observational foundations upon which this is based are comprehensive multi-band (optical and X-ray) imaging and intermediate-resolution spectroscopy going all the way out to the infall radius ($\sim 5 h_{100}^{-1}$ Mpc) for a statistically significant ($\sim$20) sample of clusters in this redshift regime. Of central importance is the use of the new 'Two Degree Field' (2dF) spectrograph facility on the $3 \cdot 9$ m Anglo-Australian Telescope (AAT) which, with its superlative ($\times$400) multiplex gain, will allow $\sim$1000 spectra to be gathered per cluster—almost an order of magnitude greater than achieved in other previous or ongoing surveys (e.g. Dressler & Schechtman 1988; the low-z component of the CNOC survey, Schade et al. 1996; Zabludoff 1998, in preparation). Hence our study will provide a significant step forward by tracking population changes not just as a function of look-back time but also as a function of the broad range of environment probed within each cluster.

Dynamical characterisation of the clusters will proceed by following and extending the technique developed by ZZ95, which combines multi-colour imaging, high-resolution X-ray imaging, and optical spectroscopy. The colour and spectral information also provides a powerful tool for quantifying the present and past star formation activity within cluster galaxies (Couch & Sharples 1987) and, in this context, the aim is to specifically look for the remnants of the blue population responsible for the Butcher–Oemler effect at higher redshifts. Our large spatial coverage will allow us to trace the variation in population characteristics from the central core—the focus of most previous studies—right out to the surrounding low-density field. The effect *local* galaxy density has on such variations, analogous to the morphology–local density relation of Dressler (1980), will also be investigated. In this context, the 250 000 galaxy spectra obtained as part of the 2dF Galaxy Redshift Survey (Colless et al. 1998)

Table 1.   Our cluster sample and its properties

Cluster	RA (1950)	Dec (1950)	z	L_{X} 10^{44} erg s^{-1}	B-M type	Richness class	CCD imagery
A0022	00 18 06·7	−26 00 00	0·1310	5·31	I	3	**B,R**
A2811	00 39 42·0	−28 49 00	0·1082	5·43	I-II	1	
A3112	03 16 11·8	−44 25 11	0·0703	7·70	I	2	**B,R**
A0550	05 50 43·6	−21 03 36	0·1251	7·06		2	**B**,R
A3378	06 04 06·2	−35 17 42	0·1410	6·87	I	1	**B,R**
A0644	08 14 58·8	−07 21 22	0·0711	7·92	III	0	**B**,R
A1084	10 42 01·5	−06 48 19	0·1346	7·42	III	0	**B**,R
A1285	11 27 49·0	−14 17 55	0·1050	5·47	II-III	1	**B**,R
A1437	11 57 51·4	+03 37 47	0·1339	7·72	I-II	3	B,R
A1650	12 56 07·0	−01 29 28	0·0845	7·81	I-II	2	B,R
A1651	12 56 47·2	−03 55 33	0·0846	8·25	I-II	1	**B**,R
A1664	13 01 00·4	−23 58 34	0·1276	5·36		2	B,R
A2055	15 16 17·3	+06 24 51	0·1021	4·78	III	0	**B,R**
A2104	15 37 28·5	−03 08 41	0·1554	7·89	III	0	**B,R**
A2204	16 30 17·6	+05 10 44	0·1524	20·58	II	3	**B,R**
A3814	21 46 12·0	−30 56 00	0·1177	3·85	II	3	
A3888	22 31 38·7	−37 59 31	0·1510	14·52	I-II	2	**B,R**,U
A3921	22 46 41·6	−64 41 47	0·0953	5·40	II	2	**B,R**,U
A2496	22 48 18·0	−16 40 00	0·1220	3·71	I-II	2	
A2597	23 22 42·0	−12 23 00	0·0852	7·97	III	0	**B,R**,U
Field 0	23 10 00·7	−12 23 48	—	—	—	—	**B,R**
Field 1	01 45 00·0	−30 00 00	—	—	—	—	**B,R**
Field 2	03 00 00·0	−36 00 00	—	—	—	–	**R**

will also provide an invaluable reference sample, particularly of the low-density field regions.

2.2 Cluster Selection

Our sample is drawn from the X-ray Brightest, Abell-type Cluster Survey (XBACS) catalogue of 242 clusters published by Ebeling et al. (1996; hereafter E96). XBACS is an X-ray follow-up of optically-selected clusters from the Abell, Corwin & Olowin (1989; ACO) catalogue. Clusters were selected from this catalogue according to the following criteria: (i) $L_{\mathrm{X}} > 3 \cdot 5 \times 10^{44}$ erg s^{-1}, (ii) $0 \cdot 07 \leq z \leq 0 \cdot 16$, (iii) Declination $< +10$ degrees, and (iv) $A_B \lesssim 0 \cdot 3$ mag (based on values from Burstein & Heiles 1984). A total of 45 clusters satisfied these criteria, from which a randomly selected subsample of 20 targets was selected; these are listed in Table 1. Column 1 lists the cluster name from the ACO catalogue; columns 2 and 3 give the Right Ascension and Declination (B1950) of the X-ray centre of the cluster respectively; column 4 lists the redshift from E96; column 5 lists the cluster's X-ray luminosity in erg s^{-1} (E96); column 6 gives the cluster's Bautz–Morgan type (ACO); column 7 lists the cluster's richness class (ACO); and column 8 denotes the filters through which the images were obtained, with those in bold face indicating cases where the data were taken in photometric conditions. It can be seen from Table 1 that our selected clusters incorporate a range of global properties such as richness class and Bautz–Morgan type. We therefore have some scope to investigate whether these properties have any bearing on the dynamical and evolutionary state of clusters.

3 Observing Strategy

3.1 CCD Imagery

The first major step of our program has been to secure high-quality, broadband B and R CCD images of each cluster in order to conduct a detailed photometric study of their galaxy populations and to identify targets for subsequent spectroscopic follow-up. Coarse morphological information on the galaxies in each cluster field is also being derived from these images. The imaging was performed at Las Campanas Observatory in Chile (LCO), using the 40 in Swope telescope equipped with a thinned 2048×2048, 24 μm pixel Tektronix CCD camera. The field of view of the CCD camera is 23′×23′, with each pixel corresponding to 0·696″ on the sky. Each cluster was imaged over a ∼2° field, thereby well encompassing its infall radius and providing coverage of the surrounding field. To image a field of this size with this instrumental set-up, a mosaic of 21 pointings (a 5×5 square without the corners; see Figure 1) was required.

For each pointing, two exposures were taken, each offset by 15 arcsec. Total combined exposure times were 600 s in the B-band and 500 s in the R-band. There was a deliberate 44 arcsec overlap between neighbouring fields in order to check and tie together the photometry and astrometry across the whole 2° field. Photometric calibration was obtained via observations of Landolt (1992) standards taken at frequent intervals between the science frames and at a variety of airmasses throughout the night. These provided both photometric zero-points for our data and measurements of the extinction coefficients on each night.
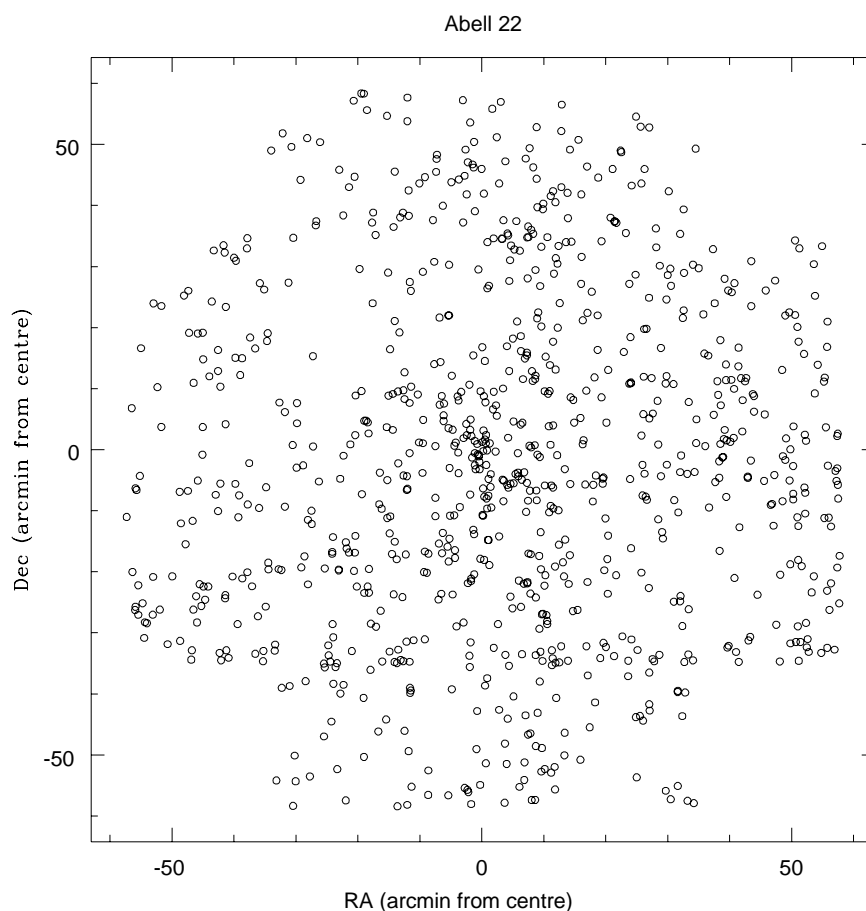
Abell 22

Figure 1—A representative image of the 2° field centred on Abell 22. The open circles represent all those galaxies in the field brighter than our spectroscopic limit of $B = 21$.

3.2 2dF Spectroscopy

The 2dF facility is ideally matched to the requirements of our study and indeed its utility in spectroscopically surveying rich clusters in unprecedented detail was a major driver in conducting this program. Its large field allows, for the first time, clusters to be easily explored right out to their infall radius. The high throughput and sensitivity of the system (with it being on a 4 m-class telescope) makes it possible to probe well down the cluster luminosity function, to a depth sufficient to detect and study any faint, remnant star-forming population. With just two 2dF configurations involving a total exposure of ~5 hr, spectra for ~760 galaxies within the field of each cluster can be obtained, realising a sample of ~400 member galaxies, a number sufficient to distinguish statistically between the properties of independent subsamples, e.g. the dynamics of star-forming versus quiescent galaxies and the higher-order kinematics of galaxies in the core and infall regions of the cluster.

The goal, therefore, is to obtain intermediate (~4 Å) resolution spectroscopy of magnitude-limited ($B \leq 21$; $M_B \sim M_B^* + 3\,\mathrm{mag}$) samples of ~760 galaxies within each cluster field, with candidates sourced from the photometric catalogues generated from our optical images (see Section 4). This spectral resolution allows both robust measurement of key absorption and emission line indices (e.g. [OII]$\lambda3727$, Ca II H & K, Hδ, Hβ) and the determination of the internal velocity dispersions of the bright, early-type cluster members. The latter provide an important additional constraint on the cluster physics through measurement of the bright-end mass function.

3.3 X-ray Imagery

Pointed observations with ROSAT using its HRI camera are being conducted to determine the distribution and morphology of the hot X-ray gas in each cluster. This will provide imagery over a 40 arcmin field of view, thereby well covering the central $2h^{-1}\,\mathrm{Mpc}$ from which most of the X-ray emission in rich clusters is seen (Fabricant et al. 1986; Evrard 1990). The ~2 arcsec spatial resolution of the ROSAT HRI will enable us to look at the intracluster medium on scales of $\sim20h^{-1}\,\mathrm{kpc}$, corresponding to that of individual galaxies. Its primary use, however, is to assess the merger history of each cluster via its morphology and its positional relation to the optical (cluster galaxy) distribution (Section 1, ZZ95).
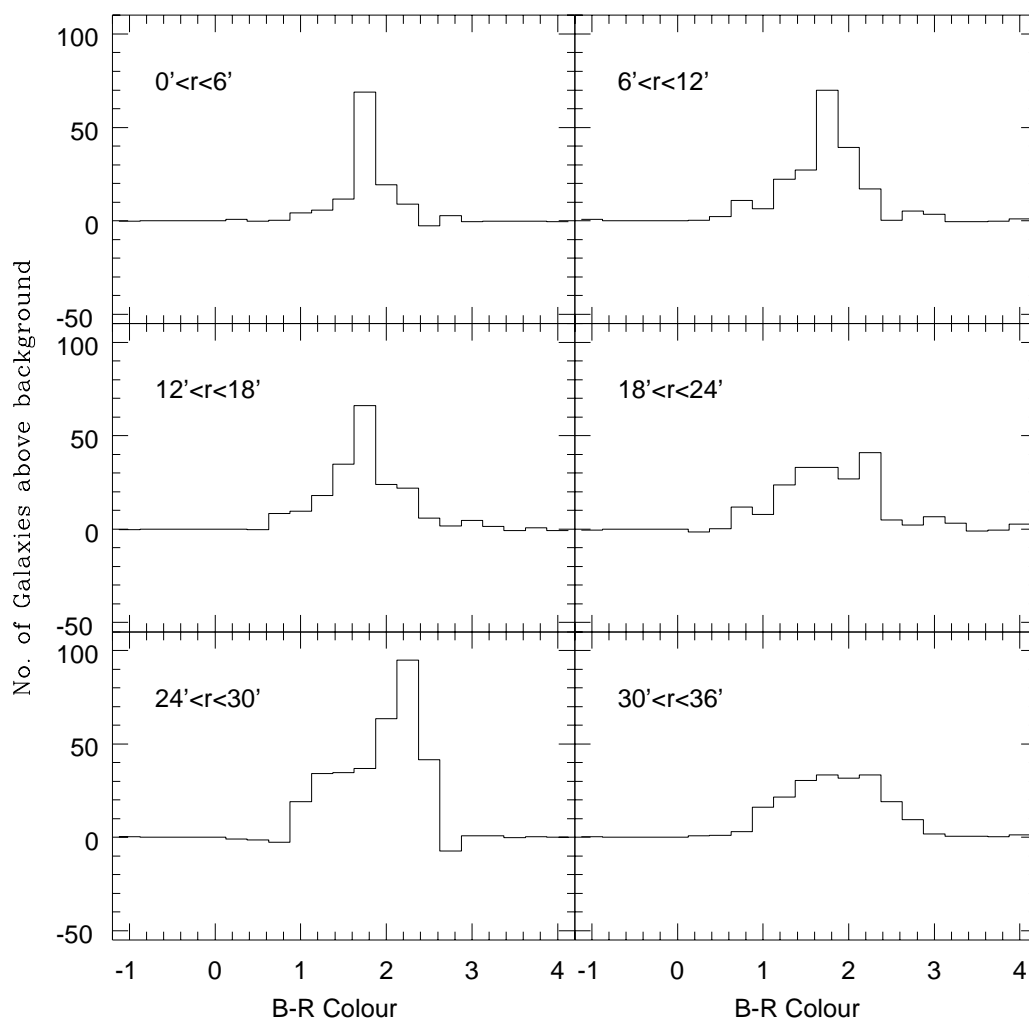
Figure 2—Field-subtracted colour histograms of galaxies down to $R = 20\cdot0$ for annuli at increasing radius from the centre of A1651.

4 CCD Imaging: First Data

The imaging component of our project is close to completion as a result of four observing runs at LCO over the period 1996 March to 1997 September. In that time, 17 clusters were imaged in both B and R, mostly in photometric conditions and in $1\cdot1$–$1\cdot5$ arcsec seeing. U-band data for a subset of clusters were also taken to better identify star-forming members. Exposures of 3 'field' regions known to be devoid of clusters (Dalton et al. 1997) were also obtained to compile a large statistical sample of field galaxies. Exposures taken in photometric conditions are indicated in Table 1. For the non-photometric cases, a series of short follow-up exposures taken in photometric conditions were obtained to ensure zero-point continuity over each cluster.

The reduction of the data has been carried out using a combination of packages in IRAF and SExtractor, the automated image analysis package, of Bertin & Arnouts (1996). The former has been used to undertake the preliminary reduction steps: The COLBIAS task was used for bias subtraction.

Images were then flat-fielded using 'super-flat' frames created by median-combining an appropriate series of program images taken on a given night. The images were then aligned and coadded using the IMALIGN and IMCOMBINE routines, with cosmic ray events and chip imperfections eliminated in the process. The detection, photometry and star/galaxy separation of objects was then done automatically on the coadded frames using SExtractor. Object identification was conducted on the R-band images using a 3σ (above sky) detection threshold within 12 or more contiguous pixels. Total magnitudes [within an aperture of radius $2\cdot5 \times r_{\mathrm{Kron}}$ see Kron (1980)]; and fixed ($4''$) aperture colours were then measured for all these objects using the R and B images. In cases where the seeing differed between the two bands, the images with the best seeing were smoothed to match those with the worst seeing before making the colour measurements. For star/galaxy separation, we used SExtractor's neural network-based algorithm.

Figure 1 shows a compilation of data from the 21 images taken of Abell 22. The open circles

represent the location of the 907 galaxies detected within the field with $B \leq 21$, our limit for 2dF spectroscopy. The check on the uniformity of our photometry facilitated by the overlap of our CCD images indicates that our magnitude and colour zero-points are stable to $\lesssim 0\cdot03$ mag across the whole $\sim 2°$ field. There is a clear overdensity of galaxies in the centre of the field, which makes up the elongated cluster core. The asymmetric distribution seen here in the core of Abell 22 is typical of many of our clusters, suggesting that the traditional assumption of a spherically symmetric galaxy distribution is the exception rather than the rule.

Field-subtracted colour distributions of galaxies in the field of Abell 1651 are shown in Figure 2. The 'field' is measured from the outskirts of the cluster itself to give a more accurate local field density subtraction. Here the data have been subdivided into annuli, each 6 arcmin in width, starting at the cluster centre and going out to a radius which encloses $\sim 90\%$ of the cluster population. Importantly, the radius of the innermost annulus corresponds to R_{30} ($0\cdot23\, h_{100}^{-1}$ Mpc at the redshift of the cluster), the standard Butcher–Oemler radius enclosing the inner 30% of the cluster population and used for measurements of blue galaxy fraction (Couch 1981; Butcher & Oemler 1984). We see there is a strong E/S0 sequence in this region of the cluster, giving rise to the dominant peak in the colour distribution at B–$R \simeq 1\cdot8$. Any population of blue galaxies, if present, would appear to be very small. There is also a conspicuous peak in the colour distribution at B–R of $2\cdot25$ within the $24' < r \leq 30'$ annulus, suggestive perhaps of a second, more distant cluster

within the $2°$ region of this field. Clearly spectroscopy is crucial for identifying blue cluster members and for detecting and eliminating contaminating objects (and members of other clusters!) within each field.

The distribution of galaxies relative to the hot X-ray gas lends insight into the complex dynamical and structural morphology of each cluster. We can easily compare these features by overlaying high resolution X-ray contours on optical images of our clusters. Figure 3 illustrates the variety in structural morphology of the central regions of clusters in our sample. The regular, concentric contours centred on the cD galaxy of Abell 3112 (Figure 3a) show that it is a relaxed cluster. There is a strong radio source also coincident with the projected position of the cD which, if it were an AGN, could have an effect on the seeming relaxedness of this cluster. However, the XBACS sample (E96) from which we drew our cluster subsample had removed all systems featuring prominent contaminating X-ray point sources, so this particular radio source does not affect the cluster X-ray map and we are indeed looking at a relaxed cluster. In cases where there is clear displacement of the cD galaxy from the X-ray centroid, the centroid is taken as the centre of mass of the cluster. Abell 3888 (Figure 3b) does not have a cD and is clearly not relaxed. There are several subclumps of galaxies and X-ray peaks and only one of the bright central galaxies coincides with a local X-ray maximum.

5 Summary

In this paper we have described a major imaging and spectroscopic survey of rich galaxy clusters at $0\cdot05 \lesssim z \lesssim 0\cdot15$ that we are currently undertaking.
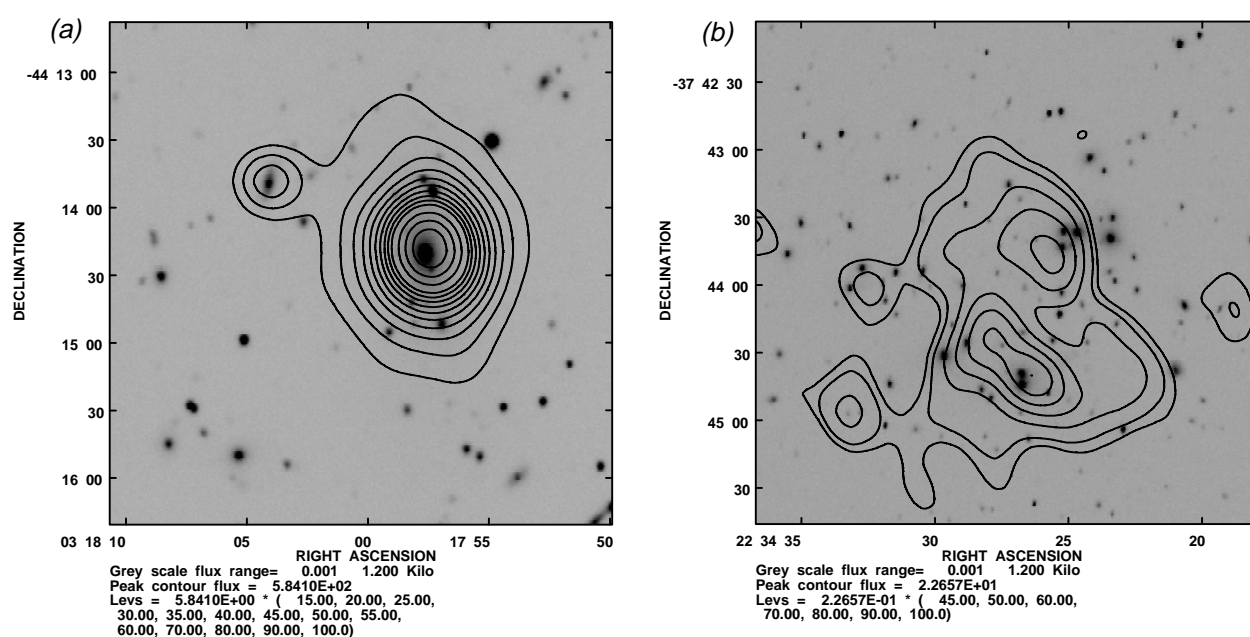

Figure 3—(a) Abell 3112 and (b) Abell 3888. The grey scale is an R-band optical image of the cluster core taken at LCO. The overlayed contours represent the ROSAT HRI X-ray images which show the gas distribution within each of the clusters.

The primary purpose of the paper has been to describe the design and scientific goals of the survey, give details of the cluster sample that we are targeting, and present some initial and very preliminary results. Publication of the major scientific results from the study must await future papers. Nonetheless, we consider this paper to serve a useful purpose in alerting other workers in the field to our study and thus perhaps focusing future observational efforts, particularly at other wavelengths (e.g. radio) on our cluster sample.

As discussed in Section 3, the optical CCD imaging component of our survey is essentially complete. The timescale for completion of the X-ray imaging and 2dF spectroscopy is another 2 years, although both are well under-way, with data collected for ∼25% of our sample. At the conclusion of the project it is our intention to make our substantial database of cluster imagery, photometry and spectroscopy publically available.

Acknowledgments

References

Abell, G., Corwin, H., & Olowin, R. 1989, ApJS, 70, 19 (ACO)

Abraham, R. G., van den Burgh, S., Glazebrook, K., Ellis, R. S., Santiago, B. X., Surma, P., & Griffiths, R. E. 1996, ApJS, 107, 1

Bahcall, N. A. 1997, to appear in Formation of Structure in the Universe, Jerusalem Winter School

Bertin, E., & Arnouts, S. 1996, A&AS, 117, 393

Burstein, D., & Heiles, C. 1984, ApJS, 54, 33

Butcher, H., & Oemler, A. 1978, ApJ, 219, 18

Butcher, H., & Oemler, A. 1984, ApJ, 285, 426

Caldwell, N., Rose, J. A., Sharples, R. M., Ellis, R. S., & Bower, R. G. 1993, AJ, 106, 473

Colless, M., et al. 1998, http://msowww.anu.edu.au/colless/2dF/ (home page of the 2dF Galaxy Redshift Survey)

Colless, M., & Dunn, A. M. 1996, ApJ, 458, 435

Couch, W. J. 1981, PhD thesis, Australian National University

Couch, W. J., & Sharples, R. M. 1987, MNRAS, 229, 423

Couch, W. J., Barger, A. J., Smail, I., Ellis, R. S., & Sharples, R. M. 1998, ApJ, 497, 188

Dalton, G. B., Maddox, S. J., Sutherland, W. J., & Efstathiou, G. 1997, MNRAS, 289, 263

Dressler, A. 1980, ApJ, 236, 351

Dressler, A. 1988, AJ, 95, 284

Dressler, A., Oemler, A, Couch, W. J., Smail, I., Ellis, R. S., Barger, A., Poggianti, B. M., & Sharples, R. M. 1997, ApJ, 490, 577

Dressler, A., & Shectman, S. A. 1988, AJ, 95, 284

Ebeling, H., Voges, W., Bohringer, H., Edge, A. C., Huchra, J. P., & Briel, U. G. 1996, MNRAS, 281, 799 (E96)

Evrard, A. E. 1990, ApJ, 363, 349

Evrard, A. E., Mohr, J. J., Fabricant, D. G., & Geller, M. J. 1993, ApJL, 419, L9

Fabricant, D., Beers, T. C., Geller, M. J., Gorenstein, P., Huchra, J. P., & Kurtz, M. J. 1986, ApJ, 308, 530.

Fort, B., & Mellier, Y. 1994, A&AR, 5, 239

Kron, R. G. 1980, ApJS, 43, 305

Lacey, C., & Cole, S. 1993, MNRAS, 262, 627

Landolt, A. U. 1992, AJ, 104, 340

Richstone, D., Loeb, A., & Turner, E. 1992, ApJ, 393, 477

Schade, D., Carlberg, R. G., Yee, H. K. C., Lopez-Cruz, O., & Ellingson, E. 1996, ApJ, 465, L103

Smail, I., Dressler, A., Couch, W. J., Ellis, R. S., Oemler, A., Butcher, H., & Sharples, R. M. 1997, ApJS, 110, 213

White, S. D. M., Briel, V. G., & Henry, J. P. 1993, MNRAS, 261, L8

Zabludoff, A. I., & Zaritsky, D. 1995, ApJL, 447, 21 (ZZ95)